Physical-Chemical Interaction in NiAl-MeB$_2$ Systems Intended for Tribological Applications

Investigation of regularities of physical-chemical interaction in the NiAl-CrB$_2$ (TiB$_2$, ZrB$_2$) systems and design of NiAl-based composite materials

BY O. UMANSKYI, O. POLIARUS, M. UKRAINETS, AND M. ANTONOV

ABSTRACT

The peculiarities of wetting and contact interaction in the NiAl-ZrB$_2$, NiAl-TiB$_2$, and NiAl-CrB$_2$ systems were studied. The investigation of contact interaction in the NiAl-MeB$_2$ (Me is Zr, Ti, or Cr) systems was carried out using a sessile drop method within the temperature range of 1650°–1670°C in a vacuum of 1.33 mPa. Contact angles for given systems proved to be 11, 20, and 0 deg, respectively. The phases and chemical compositions of the interaction products in the studied systems were determined. In the case of the NiAl-CrB$_2$ system, the formation of additional strengthening boride phase Ni-Cr-B with high hardness was identified. NiAl-15 wt-% CrB$_2$ composite material was prepared, and the microstructure and wear resistance investigated. Composites were fabricated via sintering of powder mixtures at ~1850°C in a helium atmosphere. High-temperature differential thermal analysis (HDTA) was carried out simultaneously with a sintering study. It was found that composite with CrB$_2$ proved to be almost three times more wear resistant than plain NiAl intermetallic.

KEYWORDS

• Metallide NiAl • Composite Material • Refractory Borides • CrB$_2$ • TiB$_2$ • ZrB$_2$ • Wetting • High-Temperature Differential Thermal Analysis (HDTA)

Introduction

The wide application of commercial NiAl in engine construction is based on its remarkable performance as a material for high-temperature applications (Refs. 1, 2). This remarkable performance is provided due to excellent oxidation and corrosion resistance, good thermal conductivity, high melting point, and low density of NiAl. However, tribological applications of this material are limited due to its low strength and creep resistance under high temperatures (Refs. 3–5).

It is proposed to introduce a strengthening refractory phase into the metallide NiAl and to use a dispersion strengthening mechanism to increase the deformation resistance and hardness at a high temperature in order to improve the wear resistance and widen the application range of NiAl-based materials. This may be used in order to raise the performance of engines.

In recent years, a lot of NiAl-based composite materials (CM) were developed (Refs. 5–23). The oxides and/or carbides are used as strengthening phases in these composites (Refs. 5–18). At the same time, only a few studies have been carried out concerning the tribological behavior of composite materials of NiAl-MeB$_2$ systems (Refs. 19–23). Therefore, the borides are promising candidates for high-temperature applications due to their high hardness, high corrosion, and wear resistances (Refs. 24–28).

The results of previous investigations of developed composite materials of NiAl-MeB$_2$ systems show that there is no intensive interaction between the intermetallic matrix and boride additions (Refs. 29–31). The microstructure of these materials is characterized by homogeneous distribution of the boride particles with excellent bonding to the NiAl matrix.

This work is devoted to the investigation of wetting and contact interaction in the NiAl-MeB$_2$ (Me is Zr, Ti, or Cr) systems in order to select the most appropriate strengthening of refractory phase.

Experimental Procedures

The investigation of contact interaction in the NiAl-MeB$_2$ systems was carried out using a sessile drop method within the temperature range of 1650°–1670°C in a vacuum of 1.33 mPa. Before wetting, the samples were degreased. The oxide films were removed from refractory substrates with polishing. Spreading of melt on the surface of refractory substrate was recorded with the help of a digital camera; therefore, the contact angles were determined. The process of wetting was conducted up to the achievement of the stable contact angle (for ~10 min).

The composites were fabricated via sintering of powder mixtures at ~1850°C in a helium medium. The high-temperature differential thermal analysis (HDTA) was performed simultaneously with sintering.

O. UMANSKYI, O. POLIARUS, and M. UKRAINETS (maximukrainets22@gmail.com) *are with the Frantsevich Institute for Problems of Materials Science of NASU, Ukraine. M. ANTONOV is with the Tallinn University of Technology, Estonia.*

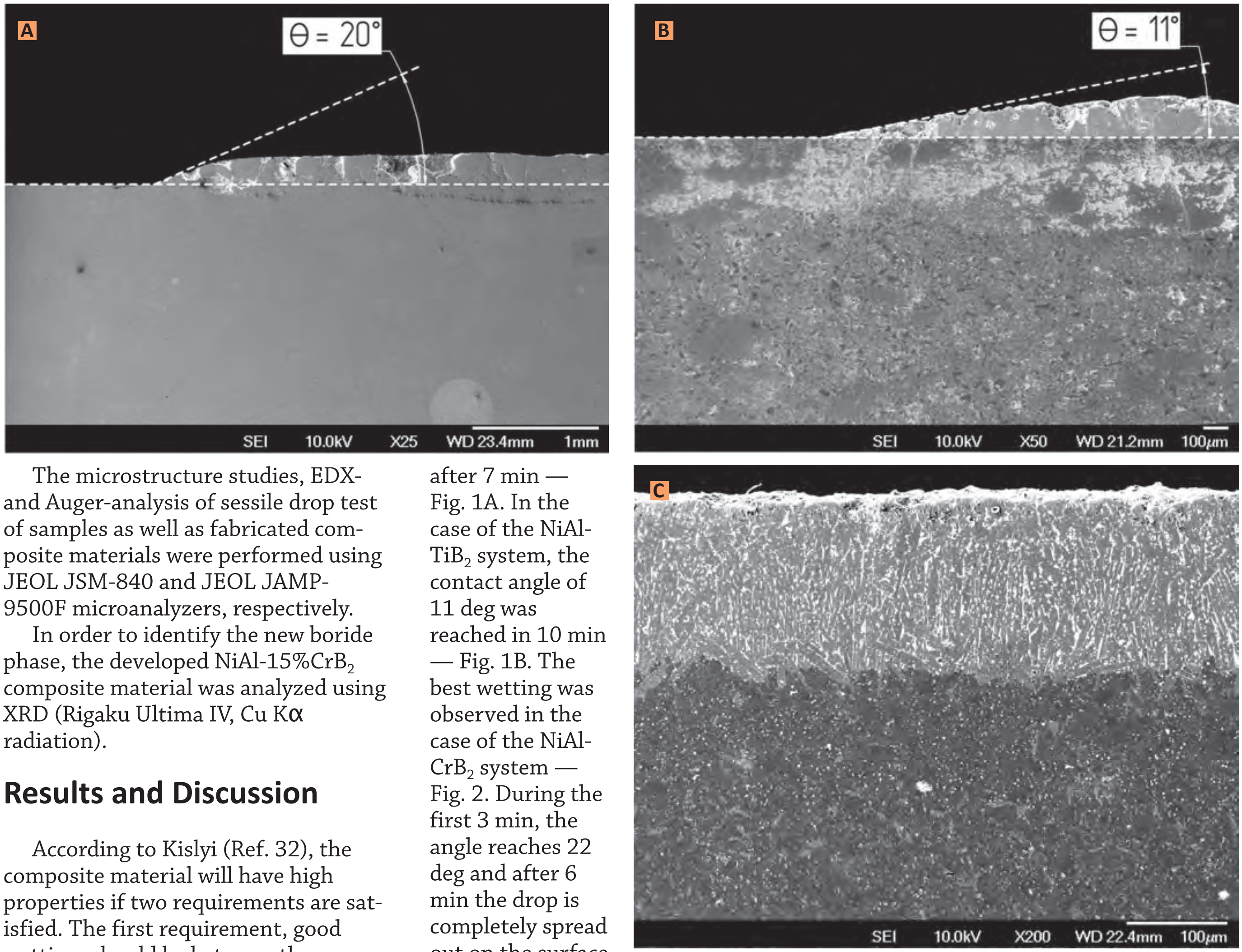

Fig. 1 — The contact angles in the NiAl-MeB$_2$ systems. A — NiAl-ZrB$_2$; B — NiAl-TiB$_2$; C —NiAl-CrB$_2$.

The microstructure studies, EDX- and Auger-analysis of sessile drop test of samples as well as fabricated composite materials were performed using JEOL JSM-840 and JEOL JAMP-9500F microanalyzers, respectively.

In order to identify the new boride phase, the developed NiAl-15%CrB$_2$ composite material was analyzed using XRD (Rigaku Ultima IV, Cu Kα radiation).

Results and Discussion

According to Kislyi (Ref. 32), the composite material will have high properties if two requirements are satisfied. The first requirement, good wetting, should be between the components of CM. The second requirement, intensive interaction between the components of composite material, which can result in formation of new phases with poor properties, should be absent. The contact (wetting) angle is the main indicator of a wetting between the components of composite material (Refs. 33, 34). Thus, determination of contact angles using the sessile drop method is the first step for the composite material development process.

The stable wetting angle of 20 deg in the NiAl-ZrB$_2$ system was recorded after 7 min — Fig. 1A. In the case of the NiAl-TiB$_2$ system, the contact angle of 11 deg was reached in 10 min — Fig. 1B. The best wetting was observed in the case of the NiAl-CrB$_2$ system — Fig. 2. During the first 3 min, the angle reaches 22 deg and after 6 min the drop is completely spread out on the surface with formation of zero contact angles — Fig. 1C.

In order to clarify the interaction between intermetallic and refractory compounds, the EDX-analysis was performed on sessile drop samples — Fig. 3.

In the interaction zone of NiAl-ZrB$_2$ samples, the identified phases corresponding to the initial components are namely ZrB$_2$ (phase 2, Fig. 3A) and NiAl (phase 1, Fig. 3A). The new phases were not observed. The depth of the transition zone proved to be 70–100 µm.

The microstructure of the interaction zone in the NiAl-TiB$_2$ system was also composed of two dominant phases, namely TiB$_2$ grains (phase 2, Fig. 3B) embedded in the NiAl melt (phase 1, Fig. 3B). The new phases were not observed.

The interaction zone was observed for the NiAl-CrB$_2$ system — Fig. 3C. The dark gray (phase 3, Fig. 3C) CrB$_2$ substrate (confirmed by EDX) had a microhardness of 19.3 GPa (Table 1).

Table 1 — Phase and Chemical Compositions of NiAl-Cr$_2$ System Interaction one (Sessile Drop Samples)

Chemical Composition, wt-% Phases	Phase Number	Ni	Cr	B	Al	Phase Compositio	Microhardness, GPa
White Phase	1	63	—	—	37	NiAl	5.7
Light Gray Phase	2	2.5	51.5	46	—	NiCrB	10.2
Dark Phase	3	0.7	46	53.3	—	CrB$_2$	19.3

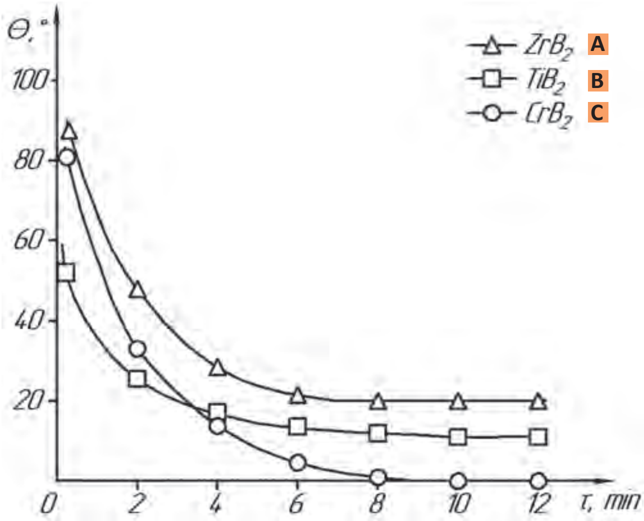

Fig. 2 — The kinetics of wetting in the NiAl-MeB$_2$ systems. A — NiAl-ZrB$_2$; B — NiAl-TiB$_2$; C — NiAl-CrB$_2$.

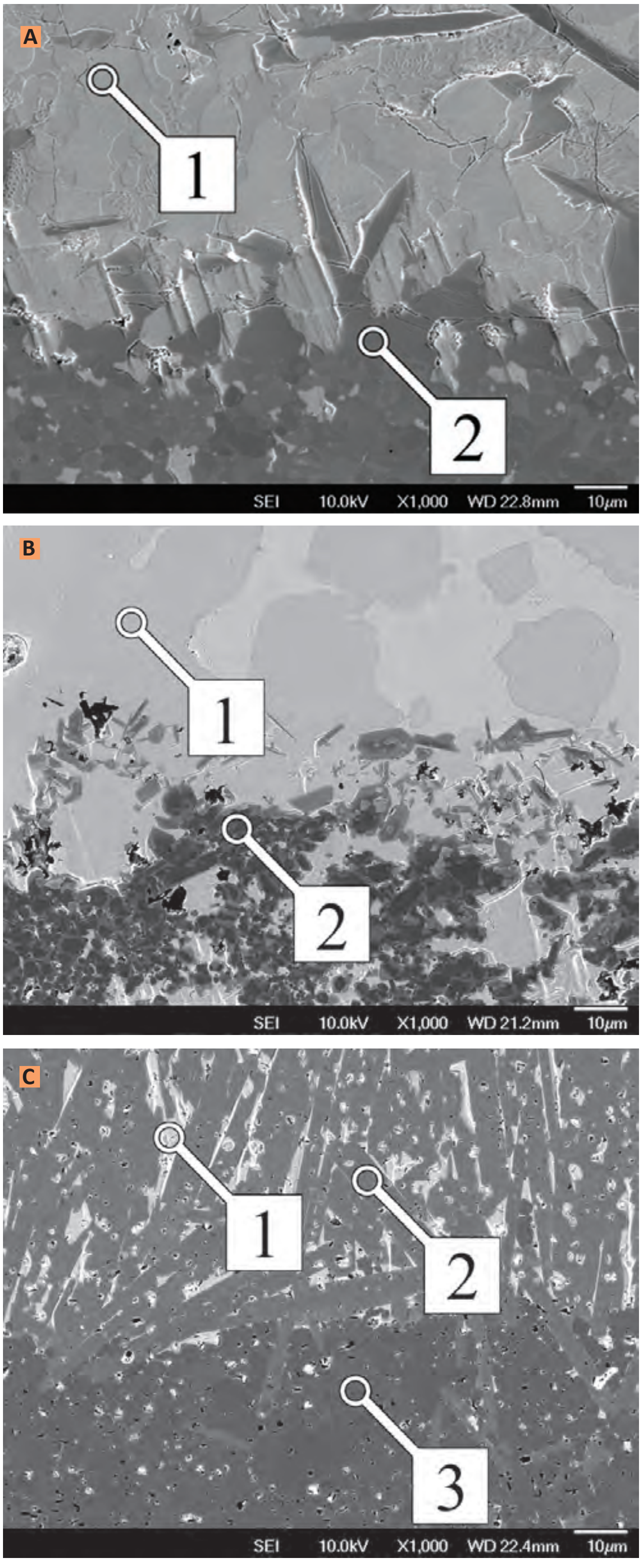

Fig. 3 — Microstructure of interaction zones. A — NiAl-ZrB$_2$; B — NiAl-TiB$_2$; C — NiAl-CrB$_2$.

The transition zone had a heterogeneous structure consisting of randomly oriented elongated light gray crystals (phase 2, Fig. 3C) embedded in a regularly distributed intermetallic phase (phase 1, Fig. 3C). The light gray crystallites of chromium boride doped with nickel (confirmed by EDX) with microhardness of 10.2 GPa (Table 1) were the products of intermetallic/chromium diboride interaction.

Formation of chromium boride phases doped with nickel was confirmed by the results of interactions in Ni-Cr-B systems investigation (Refs. 35–41). For example, a new phase, namely the CrB phase with composition $Ni_{4.66}$-$Cr_{45.52}$-$B_{45.91}$-$C_{3.91}$, was observed during the Ni-Cr-B-Si coating microstructure investigation (Ref. 35). Ni-Cr-B phases with ≥60 at-% Ni amount are called “Ni-rich boride” and phases with ≤19 at-% Ni amount called “Cr-rich boride.” These two phases were obtained by Tokoro et. al. (Ref. 37) and Yuan et al. (Ref. 40).

The formation of a new chromium boride phase doped with nickel from CrB$_2$ is shown in Fig. 4. One can see that the chromium and boron are present in the substrate (see the dark gray in lower part of Fig. 4A) and in the formed grains. A significant amount of boron is also present between the grains (see the white regions in Fig. 4A). The intensity of boron distribution evidences a difference in the chromium/boron content ratio in the substrate (bottom part of the figure) and the transition zone (Fig. 4C, D), which confirms the formation of the Ni-Cr-B phase. Nickel was found in the intergrain spaces (NiAl phase) only. The map of aluminum distribution is similar to that of nickel and is not presented — Fig. 4B.

In order to study in detail the physical and chemical compatibility of the intermetallic with borides of zirconium, titanium, and chromium, the HDTA was used for powder mixtures of NiAl-15% ZrB$_2$, NiAl-15% TiB$_2$, and NiAl-15% CrB$_2$ — Fig. 5.

High-temperature differential thermal analysis is often used for detection of the changes in the sample (either exothermic or endothermic). In our case, this technique was used for detection of quantity and temperature ranges of intensive interactions between the NiAl and borides. The upper curve of each thermogram corresponds to the heating process and the lower curve to cooling. Each of the thermogram

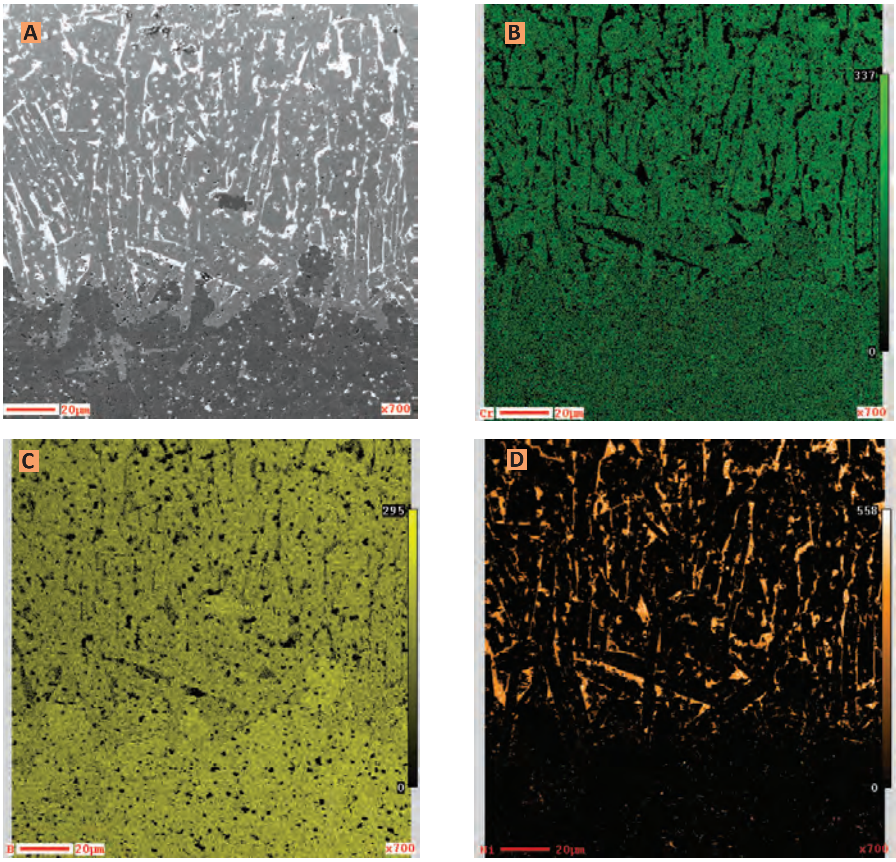

Fig. 4 — A — Structure of interaction zone in the NiAl-CrB_2 system. The following distribution can also be seen: B — Cr; C — B; D — Ni.

peaks is a result of enthalpy changing, which appears due to the processes of melting or crystallization of system components or formation of new phases.

The HDTA curves for the samples of NiAl-15% ZrB_2 (Fig. 5A) and NiAl-15% TiB_2 (Fig. 5B) are similar and characterized by the same temperature peaks (~1640°C) corresponding to melting and crystallization of the NiAl intermetallic phase. This indicates the absence of the formation of new chemical compounds in these systems.

The peculiarities of NiAl-15% CrB_2 samples (Fig. 5C) consist in the occurrence of two successive endothermic reactions at 1530° and 1638°C during heating of the powder mixtures. The first peak may be related to the formation of a new phase owing to the intermetallic/chromium diboride interaction followed by NiAl melting. Under cooling, there were observed two exothermic peaks that correspond to crystallization of the intermetallic and the new-formed phase. These results are consistent with the data obtained for the interaction contact zone in the NiAl-15% CrB_2 system — Fig. 4.

The results obtained for wetting, contact interaction, and HDTA make it evident that the most interesting system among the NiAl-MeB_2 systems is the one containing chromium diboride due to zero contact angles of wetting and formation of a new strengthening phase that can additionally give rise to the composite wear resistance.

The NiAl-CrB_2 composite materials were prepared. The initial powders of NiAl and 15 wt-% of CrB_2 were milled in a planetary mill for 6 h. Then the powders were pressed and sintered at 1700°C in a helium atmosphere. The structure of the sintered composites was composed of a light gray NiAl matrix (Fig. 6, phase 1), in which CrB_2 grains (Fig. 6, phase 2) are regularly distributed. Dark gray inclusions of chromium boride doped with nickel (Fig. 6, phase 3) are the products of the diboride/matrix interaction. According to the data of the HDTA and XRD (Fig. 7) analyses, the new chromium boride phase is the NiB/Cr_3B_4 eutectic. The obtained results are confirmed by the data of Campbell (Ref. 38), Fang (Ref. 41), and Yuan (Ref. 40).

Table 2 — Conditions of ribotestin

Load (N)	Sliding Distance (m)	Velocity (m/s)	Temperature (°C)	Counter-Body
80	1000	0.2	20	Steel Disc with NiAl Coatin

According to the EDX analysis, the composition of this new phase (in at-%) is 1.68Ni-36.89Cr-58.9B. The microhardness of Ni-Cr-B equals 9.4 GPa, somewhat between the hardess values of NiAl and CrB_2 (Table 1). The presence of such a phase additionally strengthens the composite and may positively affect the operation characteristics of this material.

The developed composite material NiAl-15%CrB_2 and plain metallide NiAl were subjected to comparative tribotechnical tests according to "pin-on-disc" configuration using a friction machine CETR (now Bruker) UMT-2 (Table 2). The tests showed that introduction of chromium diboride into the metallide has positive effect and leads to an increase in the wear resistance by 2.9 times in comparison with that of NiAl in dry friction conditions — Fig. 8.

Conclusion

In order to justify the selection of strengthening phase for NiAl-based composites aiming to raise the wear resistance, the peculiarities of wetting and contact interaction in the NiAl-ZrB_2, NiAl-TiB_2, and NiAl-CrB_2 systems have been studied.

It has been found that the most promising strengthening phase is chromium diboride since the wetting in the NiAl-CrB_2 system is characterized by zero angle. As the result of interphase interaction, the Ni-Cr-B phase is formed, which may be considered as an additional strengthening agent for the composites.

The novel composite material, NiAl-15%CrB_2, was developed.

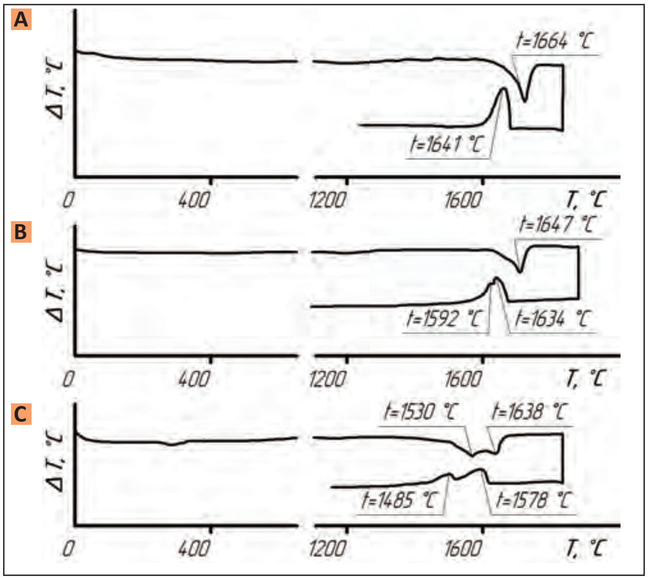

Fig. 5 — Chemical interaction in the NiAl-MeB$_2$ systems. A — NiAl-15% ZrB$_2$; B — NiAl-15% TiB$_2$; C — NiAl-15% CrB$_2$.

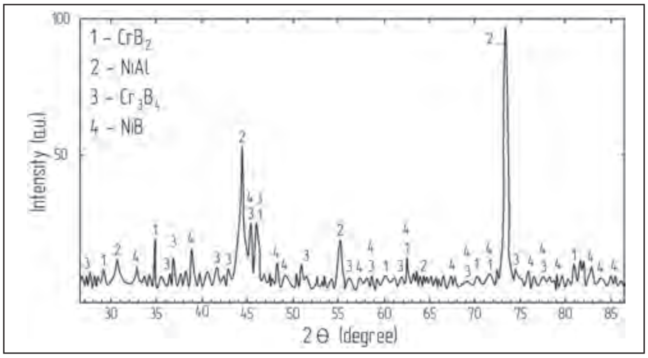

Fig. 7 — XRD pattern of the NiAl-15%CrB$_2$ composite material.

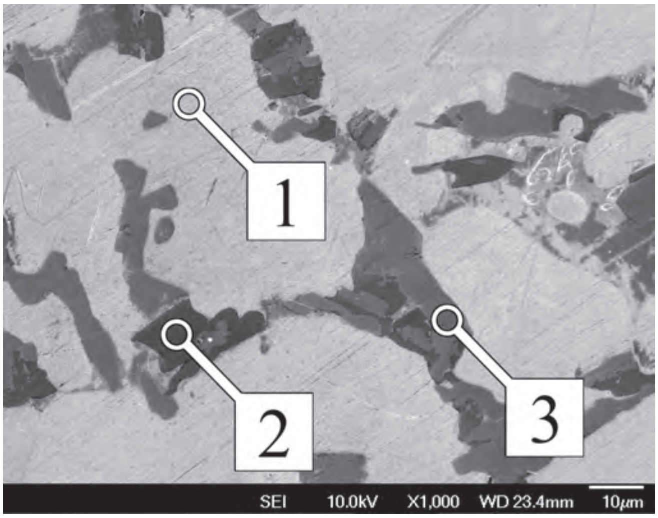

Fig. 6 — Microstructure of the NiAl-15% CrB$_2$ composite material.

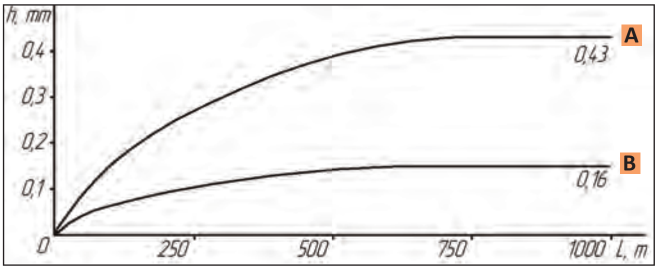

Fig. 8 — Wear of pins depending on the sliding distance. A — Intermetallic NiAl; B — composite NiAl-15% CrB$_2$.

References

1. Bolshakov, V., Kharchenko, V., Zhuravel, V., Zahorodnyi, A., Liubushkin, V., Zamrkovoi, V., and Miloserdov, A. 2008. Investigation of heat protective running-in coatings for turboprop engine retainers – Part 1. *Construction, Materials Science, Mechanical Engineering: Sat Scientific Works* 45: 87–91.

2. Migunov, V., Farafonov, D., Dehovets, M., and Stupina, T. 2012. Sealing materials for gas flow regions of turbine engines. *Aviation Materials and Technologies*: 9.

3. Westbrook, J. H., and Fleischer, R. L. 2000. NiAl and its alloys. *Intermetallic Compounds. Structural Applications of Intermetallic Compounds*. Vol. 3, p. 346. New York, N.Y.: Wiley.

4. Umanskyi, A., Poliarus, E., Kostenko, A., and Terentyev, A. 2012. Effect of the nickel metallide based coating composition on the mechanisms of wear under conditions of high temperature tribological tests. *Tribology Problems* 3: 123–127.

5. Guo, J., Wang, Z., Sheng, L., Zhou, L., Yuan, C., Chen, Z., and Song, L. 2012. Wear properties of NiAl based materials. *Progress in Natural Science: Materials International* 22(5): 414–425.

6. He, L., Tan, Y., Wang, X., Tan, H., and Zhou, C. 2014. Tribological properties of WC and CeO$_2$ particles reinforced in-situ synthesized NiAl matrix composite coatings at elevated temperature. *Surface & Coatings Technology* 244: 123–130.

7. Karantzalis, A. E., Lekatou, A., and Tsirka, K. 2012. Solidification observations and sliding wear behavior of vacuum arc melting processed Ni–Al–TiC composites. *Materials Characterization* 69: 97–107.

8. Liu, E., Gao, Y., Jia, J., Bai, Y., and Wang, W. 2014. Microstructure and mechanical properties of in situ NiAl–Mo$_2$C nanocomposites prepared by hot-pressing sintering. *Materials Science & Engineering A* 592: 201–206.

9. Mohammadnezhad, M., Shamanian, M., Enayati, M. H., Salehi, M., and Hoseynian, A. 2014. Microstructures and properties of NiAl–TiC nanocomposite coatings on carbon steel surfaces produced by mechanical alloying technique. *Surface & Coatings Technology* 238: 180–187.

10. Movahedi, B. 2013. Fracture toughness and wear behavior of NiAl-based nanocomposite HVOF coatings. *Surface & Coatings Technology* 235: 212–219.

11. Sheng, L. Y., Yang, F., Xi, T. F., and Guo, J. T. 2013. Investigation on microstructure and wear behavior of the NiAl–TiC–Al$_2$O$_3$ composite fabricated by self-propagation high-temperature synthesis with extrusion. *Journal of Alloys and Compounds* 554: 182–188.

12. Sheng, L. Y., Yang, F., Guo, J. T., Xi, T. F., and Ye, H. Q. 2013. Investigation on NiAl–TiC–Al$_2$O$_3$ composite prepared by self-propagation high temperature synthesis with hot extrusion. *Composites: Part B* 45: 785–791.

13. Sheng, L. Y., Guo, J. T., Xi, T. F., Zhang, B. C., and Ye, H.Q. 2012. ZrO$_2$ strengthened NiAl/Cr (Mo,Hf) composite fabricated by powder metallurgy. *Progress in Natural Science: Materials International* 22(3): 231–236.

14. Shi, X., Wang, M., Zhai, W., Zhu, Z., Xu, Z., Zhang, Q., Song, S., Yao, J., and Qamar ud Din, A. 2013. Friction and wear behavior of NiAl–10 wt%Ti$_3$SiC$_2$ composites. *Wear* 303: 9–20.

15. Shi, X., Wang, M., Zhai, W., Xu, Z.,

Zhang, Q., and Chen, Y. 2013. Influence of Ti_3SiC_2 content on tribological properties of NiAl matrix self-lubricating composites. *Materials and Design* 45: 179–189.

16. Shi, X., Zhai, W., Xu, Z., Wang, M., Yao, J., Song, S., and Wang, Y. 2014. Synergetic lubricating effect of MoS_2 and Ti_3SiC_2 on tribological properties of NiAl matrix self-lubricating composites over a wide temperature range. *Materials and Design* 55: 93–103.

17. Shi, X., Zhai, W., Wang, M., Xu, Z., Yao, J., Song, S., and Wang, Y. 2014. Tribological behaviors of NiAl based self-lubricating composites containing different solid lubricants at elevated temperatures. *Wear* 310: 1–11.

18. Zhu, S., Bi, Q., Niua, M., Yanga, J., and Liua, W. 2012. Tribological behavior of NiAl matrix composites with addition of oxides at high temperatures. *Wear* 274-275: 423–434.

19. Ukrainets, M., Umanskyi, O., Poliarus, O., Kuschev, O., and Stel'mah, O. 2013. The tests temperature influence on tribological characteristics of NiAl-CrB_2 composite coatings. *Research Notes* 41, Part 2: 206–212.

20. Umanskyi, O., Poliarus, O., Ukrainets, M., and Martsenyuk, I. 2014. Effect of ZrB_2, CrB_2 and TiB_2 additives on the tribological characteristics of NiAl-based gas-thermal coatings. *Key Engineering Materials* 604: 20–23.

21. Riga. RTU. 2013. Influence of CrB_2 additives into NiAl intermetallics on tribological properties of thermal spray coatings at high temperature friction. *Proc. Conf. MET-2013: Mat., Environment, Tech*. Eds. O. Umanskyi, O. Poliarus, M. Ukrainets, O. Kostenko, and O. Terentyev, pp. 37–43.

22. Umanskyi, O., Poliarus, O., Kostenko, O., and Ukrainets, M. 2014. Influence of refractory borides additives on wear mechanism of plasma spraying coatings based on NiAl intermetallic. *Problems of Tribology* 1: 46–52.

23. Umanskyi, O., Poliarus, O., Ukrainets, M., Dovgal, A., Kapitanchuk, L., and Subbotin, V. 2013. The structure and properties investigations of composite materials and coatings based on NiAl-TiB_2 systems. *Aerospace Technic and Technology* 10(107): 20–24.

24. Lofaj, F., Mikula, M., Grančič, B., Cempura, G., Horňák, P., Kúš, P., and Kottfer, D. 2011. Tribological properties of TiBx and WC/C coatings. *Ceramics – Silikáty* 55(4): 305–311.

25. Senda, T., Yamamoto, Y., and Ochi, Y. 1993. Friction and wear test of titanium boride ceramics at elevated temperatures. *Journal of the Ceramic Society of Japan* 101(4): 461–465.

26. Xiao, H., Yin, J., and Senda, T. 2007. Tribology of titanium boride sliding against silicon carbide at elevated temperatures. *Key Engineering Materials* 353–358: 1580–1583.

27. Justin, J. F., and Jankowiak, A. 2011. Ultra-high temperature ceramics: densification, properties and thermal stability. *The Onera Journal AerspaceLab* 3 AL03-08: 1–11.

28. Eakins, E., Jayaseelan, D. D., and Lee, W. E. 2011. Toward oxidation-resistant ZrB_2-SiC ultra high temperature ceramics. *Metallurgical and Materials Transactions A* 42A: 878–887.

29. Cui, H., Ma, L., Cao, L., Teng, F., and Cui, N. 2014. Effect of NiAl content on phases and microstructures of TiC–TiB_2–NiAl composites fabricated by reaction synthesis. *Trans. Nonferrous Met. Soc. China* 24: 346–353.

30. Erdem Camurlu, H., and Maglia, F. 2009. Self-propagating high-temperature synthesis of ZrB_2 or TiB_2 reinforced Ni–Al composite powder. *Journal of Alloys and Compounds* 478: 721–725.

31. Shokati, A. A., Parvin, N., and Shokati, M. 2014. Combustion synthesis of NiAl matrix composite powder reinforced by TiB_2 and TiN particulates from Ni–Al–Ti–BN reaction system. *Journal of Alloys and Compounds* 585: 637–643.

32. Kislyi, P. 1985. *Cermets*. 272, Kyiv, Naukova dumka.

33. Shafrin, E. G., and Zisman, W. A. 1960. Constitutive relations in the wetting of low energy surfaces and the theory of the retraction method of preparing monolayers. *J. Phys. Chem*. 64(5): 519–524.

34. Delannay, F., Froyen, L., and Deruyttere, A. 1987. The wetting of solids by molten metals and its relation to the preparation of metal-matrix composites. *J. Mater. Sci*. 22: 1–16.

35. Xuan, H., Wang, Q., Bai, S., Liu, Z., et al. 2014. A study on microstructure and flame erosion mechanism of a graded Ni–Cr–B–Si coating prepared by laser cladding. *Surf. Coat. Technol*. 244: 203–209.

36. Bondar, A. 2007. Non-ferrous metal systems. Part 3/M.S.I.T. MSIT® // Non-Ferrous Metal Ternary Systems. Selected Soldering and Brazing Systems: Phase Diagrams, Crystallographic and Thermodynamic Data. Springer-Verlag. T. 11C3–C. 153–159.

37. Tokoro, K., Wikstrom, N. P., Ojo, O. A., and Chaturvedi, M. C. 2008. Variation in diffusion-induced solidification rate of liquated Ni–Cr–B insert during TLP bonding of Waspaloy superalloy. *Mater. Sci. Eng. A* 477: 311–318.

38. Campbell, C. E., Kattner, U. R., and Division, M. 2002. Assessment of the Cr-B system and extrapolation to the Ni-Al-Cr-B quaternary system. *Calphad*. 26, 3: 477–490.

39. Liu, J., Jin, T., Zhao, N., Wang, Z., Sun, X., Guan, H., and Hu, Z. 2011. Microstructural study of transient liquid phase bonded DD98 and K465 superalloys at high temperature. *Mater. Charact*. 62, 5: 545–553.

40. Yuan, X., Kim, M. B., and Kang, C. Y. 2009. Characterization of transient-liquid-phase-bonded joints in a duplex stainless steel with a Ni–Cr–B insert alloy. *Mater. Charact*. 60, 11: 1289–1297.

41. Fang, J., Chen, X., Liu, B., Yan, S. et al. 2005. Liquid-phase chemoselective hydrogenation of 2-ethylanthraquinone over chromium-modified nanosized amorphous Ni–B catalysts. *J. Catal*. 229: 97–104.
